

Chapter 1

Introduction

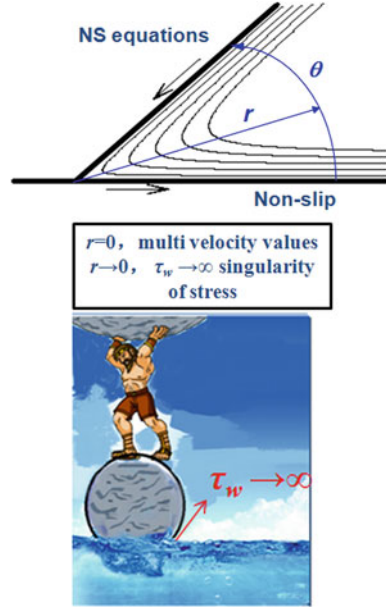
Abstract This chapter describes the importance of dynamic wetting research and its application in modern industry. Some important physical concepts and principles involved in dynamic wetting phenomena have been reviewed. This chapter also reviews and summarizes the new achievements and contributions of recent investigations in the topics of dynamic wetting by complex fluids. The latest development on the research of nanofluid dynamic wetting is also described. In the last part of this chapter, the research roadmap of this book is provided.

1.1 Backgrounds

Dynamic wetting is a process that one fluid replaces the other fluid on the solid surfaces, which is a very common natural phenomenon. The dynamic wetting is widely involved in our daily activities and industrial applications. There are many examples of wetting in our daily life: the morning dew hanging on the grass, the rain drops rolling on the windows, the coffee staining the table, the water rising in the capillaries of a tree. The dynamic wetting also takes place in many industrial processes, such as coating, oil exploration, film manufacturing, printing, food production, dyeing, and mineral flotation. In thermal engineering, the flow and phase change of working mediums are two fundamental processes in many energy convert and thermal management devices. The dynamic wetting, which relates to the fluid flow and phase-change behaviors, plays significant roles in these energy utilization systems. Particularly, the dynamic wetting is very important in various microfluidic systems, such as the microchips or biochips, in which the surface tension plays significant roles when the system size reduces.

The contact line motion is the core problem that dynamic wetting deals with. The relationship between the dynamic contact angle and the contact line velocity (θ_D-U), as well as the relationship between the spreading radius and the spreading time ($R-t$), is usually used to describe the dynamic wetting of fluids on solid surfaces. These two relationships not only present the wettability of the fluids on the

Fig. 1.1 Schematic of “contact line paradox”



solid surfaces, but also show the energy dissipation mechanisms during the dynamic wetting process [1–4]. The time-dependent dynamic wetting is of great practical interest because fluids are usually used in flow devices. The dynamic wetting process can be divided into two categories: the forced wetting and the spontaneous wetting. In the forced wetting, the contact line motion is triggered by the external forces, for example, the dynamic wetting of fluid in the capillary tube is driven by the external pressure; the other example is the electrowetting, which is driven by the external electricity field. In the spontaneous wetting, the dynamic wetting takes place without any external forces (except the gravity). The droplet spreads outwards to reduce the contact angle to reach the equilibrium stage with the lowest systemic free energy, corresponding to the equilibrium contact angle.

The dynamic wetting process looks very simple. However, complexity always hides beneath the simplicity. The complication of dynamic wetting process lies in several facts: (1) The process is driven by multiple driven forces, such as viscosity force, inertial force, gravity, and capillary force; (2) the process is affected by various properties of spreading fluids, such as surface tension, viscosity, or rheology; (3) the process is also sensitive to various solid surface properties, such as surface roughness, porosity, or surface charge; (4) the process usually occurs with complex external physical fields, such as electricity field, magnetite field, or thermal field. The complexity of dynamic wetting also lies in the famous “contact line paradox” or “stress singularity” [2]. As shown in Fig. 1.1, if we solve the flows near the contact line region, using the classical Navier–Stokes (NS) equations and the

non-slip boundary conditions, we will obtain an infinite force acting at the three-phase contact line. With such an infinite force, the contact line cannot move. However, the dynamic wetting process always takes place spontaneously in nature. Therefore, “not even Herakles could sink a solid if the physical model were entirely valid” [2]. The “contact line paradox” was initially proposed by Huh and Scriven in 1971 and drew extensively research interests on this topic. However, the mystery is still waiting for being unveiled up to now.

Recently, the researchers have paid widely attentions in nanofluid dynamic wetting. Adding nanoparticles into base fluids can greatly change the thermal conductivity, thermal diffusion coefficient, or phase-change behaviors. Therefore, nanofluids have been regarded as one of the promising heat transfer enhancement technologies. Nanofluids have been reported to increase the boiling heat transfer coefficient or critical heat flux (CHF) value, and hence preventing the boiling crisis. The improvement in the nanofluid boiling is not only attributed to the modification of thermal properties, but also to the dynamic wetting behaviors. The special dynamic wetting properties of nanofluids can provide us with a new approach to control the fluid wetting process, with which the solid–liquid wettability can be tuned from the aspect of fluids rather than solid surfaces. The advantage of the tuning the wettability using nanofluids lies in the multiformity of nanofluids, because there are many tunable parameters in nanofluids, such as nanoparticle material, shape, diameter, loading fraction, wettability, as well as base fluid. The tunable nanofluid dynamic wetting behaviors extend the potential applications of nanofluids to many scientific and engineering areas. For example, we can manipulate the nanoparticle self-assembly with the tunable nanofluid wettability. Then, we can fabricate the functional surfaces with desired physical, chemical, or optical characteristics, such as super-hydrophobic or super-hydrophilic surfaces, invisible coating on the fighter surfaces. Nanofluids are also widely involved in the bio/medicine engineering. The dynamic wetting plays a key role in the transport of bio/medicine nanoparticles in the biochips or other microfluidic devices.

For nanofluids, the additional nanoparticles induce the complex particle–particle and particle–solvent molecule interaction, which makes the dynamic wetting by nanofluids more complex. As shown in Fig. 1.2, the study of nanofluid dynamic wetting encounters two tremendous challenges. The first one is the lack of nanoscale experimental technique or theoretical description of complex nanoparticle random motion, sedimentation, or self-assembly. In addition, the dynamic wetting of nanofluids was a combination process governed by multiple forces. These forces cross several length scales, from 10^{-3} to 10^{-9} m. The lack of multi-scale or cross-scaled experimental technique or theoretical description also prevents the well understanding of the mechanisms of nanofluid dynamic wetting.

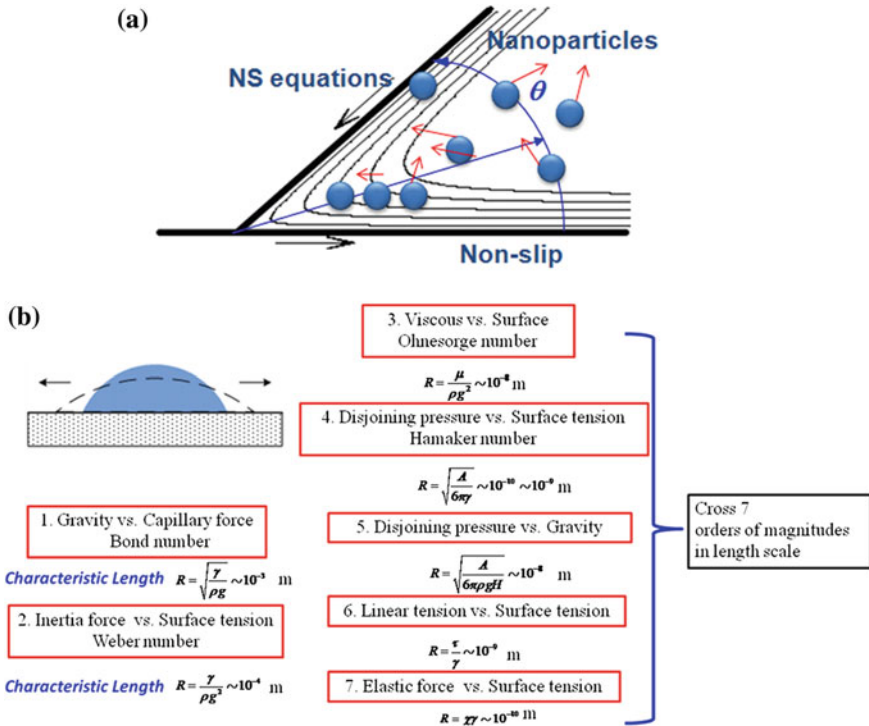


Fig. 1.2 Two tremendous challenges lie in the study of nanofluid dynamic wetting. **a** The nanoscale nanoparticle motions and the solid–liquid interaction. **b** Multiscale and cross-scaled characteristics

1.2 Literature Review


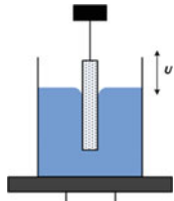
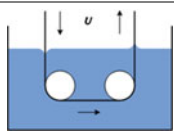

1.2.1 Dynamic Wetting of Newtonian Fluids

In order to reveal the complex dynamic wetting phenomenon, the early studies mainly focused on the simple fluids and ideal solid surfaces without considering the roles of any external physical fields. Extensive experiments [5–13], theories [14–42], and numerical simulations [43–62] have been conducted to reveal the fundamental mechanisms of the dynamic wetting by Newtonian fluids.

Among the experiments, several experimental techniques have been developed to measure the dynamic contact angle and the spreading radius during the dynamic wetting process, such as droplet spreading, Wilhelmy plate dipping, plunging tape, and capillary tube [5], which are summarized in Table 1.1.

Among the theoretical works, the dynamic wetting of Newtonian fluids has been studied extensively in last five decades. The motivations of the early study mainly focused on the “contact line paradox” issue or the physical mechanism of contact

Table 1.1 Experimental techniques in the dynamic wetting

Methods	Schematic	Wetting modes	Parameters	Fundamental
Droplet spreading		Spontaneously wetting	$R - t;$ $\theta_D - U$	Optical method
Wilhelmy plate dipping		Forced wetting	$\theta_D - U$	Mechanical method
Plunging tape		Forced wetting	$\theta_D - U$	Optical method
Capillary tube		Forced wetting	$\theta_D - U$	Optical method

line movement. One general approach among these studies was using slip boundary condition rather than non-slip condition to remove the stress singularity. The paradox was solved by the math, but not by the physics. The physical connotation of contact line movement is still beyond the satisfactory explanation [15–20]. Another way to remove the stress singularity was using a hypothetical monomolecular thin-film layer ahead of the nominal contact line moving on the solid surface, which was known as precursor layer. The singularity point was removed to infinite far away by the precursor layer from the apparent contact line. Therefore, the “contact line paradox” can be avoided [21–23].

By introducing various microscopic hypotheses to remove the stress singularity at the contact line, several theoretical models have been established to describe the dynamic wetting process of Newtonian fluids. Among these models, the hydrodynamic model (HD) [15–23] and the molecular kinetic theory (MKT) [24] are most influential.

In HD, the “stress singularity” is assumed to only occur in the microregion near the contact line. In this region, continuous assumptions are no longer held due to the modification of fluid microscopic properties by the solid surface microstructure, the fluid heterogeneity, or the non-Newtonian effects. Therefore, the traditional NS equations with classical non-slip boundary conditions fail to describe the flows in this region. Additional microscopic assumptions, such as the precursor layer, slip boundary, or shear-thinning non-Newtonian conditions are needed to solve the flow fields. The evolution of droplet shape, dynamic contact angle, and the contact line moving velocity can be derived from the HD.

Another popular model is called MKT, which completely abandons the continuous assumptions in the NS equations and seeks a new approach to describe the

contact line motion problems. In MKT, the principal hypothesis is that the motion of the three-phase line is ultimately determined by the statistical kinetics of molecular adsorption/desorption events occurring within the three-phase zone. For the contact line to advance, a forward-direction shear stress to the molecules within three-phase zone modifies the profiles of the potential energy barriers to molecular displacements in the forward direction. Therefore, the displacements in the forward direction are more frequent than those in the reverse direction, leading to the advancing of contact line.

Both of these models contain several microscopic parameters, such as the slip length, L_s , in the HD model; the molecular displacement frequency, K ; and the displacement distance, λ , in the MKT model. These parameters are immeasurable, but can be fitted from the macroscopic dynamic wetting data, such as $\theta_D - U$ and $R - t$. Therefore, the experimental dynamic wetting data can provide us a tool to look inside the microscopic pictures in the microzone of contact line region.

The typical dynamic wetting models of Newtonian fluids are listed as follows.

1. Hydrodynamic model

The HD can be divided into two categories: one is purely hydrodynamic approach (PHA) or standard hydrodynamic approach, which is strictly derived from the momentum equations; the other is energy-balanced approach (EBA), in which the dynamic wetting is considered as an energy dissipation process [25]. The typical HDs of Newtonian fluids were summarized in Table 1.2.

2. Molecular kinetic model

Figure 1.3 illustrates the molecular displacement near the contact line region in the MKT model [24, 35, 36]. The absorbed sites locate randomly on the initial solid-liquid interface. The liquid molecular replacements occur randomly but progressively within the moving three-phase contact line zone. At equilibrium, the molecular displacement frequency in the forward direction equals to the frequency in the backward direction. However, when the contact angle diverges from the equilibrium value, the contact line movement is triggered by the unbalanced Young's stress, $F_Y = \sigma_{LV}(\cos \theta_0 - \cos \theta_D)$. Young's stress

Table 1.2 Typical hydrodynamic models of Newtonian fluids

Authors	Model	Equation	Description
Dussan [18]	PHA	$G(\theta_D) = G(\theta_{cl}) + Ca \ln\left(\frac{L_H}{L_S}\right)$	Two zones
Cox [26]	PHA	$G(\theta_D) = G(\theta_{cl}) + Ca \left[\ln\left(\frac{L_H}{L_S}\right) + \frac{Q_{in}}{f(\theta_{cl})} - \frac{Q_{out}}{f(\theta_D)} \right]$	Three zones
Zhou and Sheng [27, 28]	PHA	$G(\theta_D) = G(\theta_{cl}) + 9Ca \left[\ln\left(\frac{L_H}{L_S}\right) + C_{ZS} \right]$	Slip length normalization
de Gennes [1, 31], Brochard-Wyart [32, 33]	EBA	$\theta_D(\theta_D^2 - \theta_0^2) = 6Ca \ln\left(\frac{L_H}{x_m}\right)$	Young unbalanced force and viscous dissipation

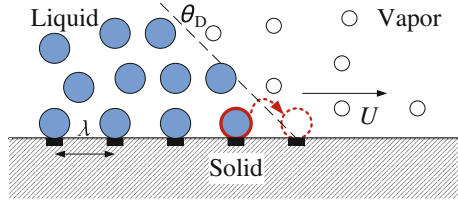


Fig. 1.3 Schematic of molecular displacement near the contact line region in MKT model [35]

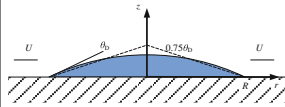
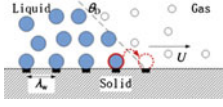
modified the profiles of the potential energy barriers to molecular displacement, lowering the barriers in the forward direction and raising those in the backward direction. Consequently, the molecular displacements in the forward direction become more frequent than those in the reverse direction, leading to the contact line motion in the macroscopic scale. The contact line velocity is related to the displacement frequency K and the average distance between the two adsorption sites, λ , which gives $U = K\lambda$. Therefore, we have the relation of the dynamic contact angle and the contact line velocity,

$$\cos \theta_D = \cos \theta_0 - \frac{2k_B T}{\sigma_{LV} \lambda^2} \operatorname{arcsinh} \left(\frac{U}{2K\lambda} \right), \quad (1.1)$$

in which θ_0 is the equilibrium contact angle, θ_D is the dynamic contact angle, k_B is Boltzmann constant, σ_{LV} is the liquid–vapor surface tension, K is the molecular displacement frequency, λ is the average distance of molecular displacement.

The advantage of MKT lies in its microscopic instinct in the explanation of contact line motion, without the help of slip hypothesis. In addition, the solid surface characteristics can be considered in the model. However, the model does not consider the viscous effects. The two models provide two explanations from different aspects to the contact line motion. In the HD model, the energy dissipation during the dynamic wetting occurs in the bulk droplet, referred to as the bulk dissipation or the viscous dissipation. In this model, the apparent contact angle is defined by either the outer region angle or the included angle that the moving meniscus extends to the solid–liquid interface. However, in the MKT model, the energy dissipation taking place in the vicinity of contact line zone dominates the spreading energy dissipation process, which is known as the local dissipation. The moving meniscus is determined by Young–Laplace equation. Therefore, the macroscopic contact angle in the MKT is strictly defined. It should be noted that there is still controversy whether λ depending on the liquid properties or solid surface properties in MKT [8, 38, 39]. Blake, who initially proposed the theory, claimed that the parameter λ might depend on the molecular size, but is determined, to a much greater extent, by the distance of the absorption sites on the solid surface [36]. The MKT model has been widely applied in the Newtonian fluid dynamic wetting process [36–40].

Table 1.3 Comparison of two dynamic wetting models

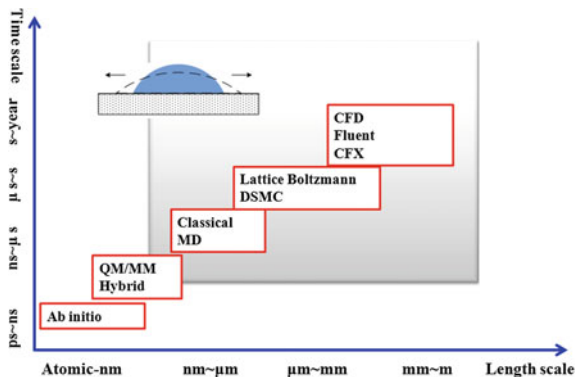
	Hydrodynamic model	MKT model
Physical scenario		
Fundamental theory	Lubrication approximation	Eyring theory
Parameters	p, U, Ca, θ, L_H	λ, K, U, θ, G
Equations	$\theta_D (\theta_D^2 - \theta_0^2) = 6Ca \ln \left(\frac{L_H}{x_m} \right)$	$\cos \theta_D = \cos \theta_0 - \frac{2k_B T}{\sigma_{LV} \lambda^2} \operatorname{arcsinh} \left(\frac{U}{\sqrt{2K\lambda}} \right)$
Microscopic parameters	x_m, L_s	λ, K
Dissipation mode	Viscous dissipation	Local dissipation
Scope of application	Small contact angle	Large contact angle

The two typical models provide the understanding of contact line motion from different aspects, and also provide good agreement with most experimental data. However, both models have their limitations in the scope of application. In addition, they both contain unmeasured microscopic parameters. Table 1.3 compares the two typical dynamic wetting models.

The spreading law, the relation of spreading radius versus spreading time, is another research topic in the dynamic wetting. The spreading law has been established for the complete wetting of Newtonian fluids. The spreading radius is expressed as the power law of spreading time, $R(t) \sim at^\alpha$, in which α is the spreading exponent. The exponent is used to characterize not only the contact line velocity, but also the energy dissipation mode during the contact line moving. In HD models, in which the viscous dissipation dominates, $\alpha = 1/10$ for the capillary regime, while $\alpha = 1/8$ [22] for the gravitational regime. However, $\alpha = 1/7$ for the MKT model [15], in which the local dissipation dominates. The unique spreading law fails in the partial wetting cases. de Ruijter et al. [10] suggested that the partial wetting process can be divided into three stages: the early spreading stage with $R(t) \sim R_0 + at$, the middle stage with $R(t) \sim t^{0.1}$, and the last stage when the dynamic contact angle approaching the equilibrium contact angle, which gives $\Delta R(t) \sim \exp(-t/T)$, in which $\Delta R(t) = R_{\text{eq}} - R(t)$, T is a constant. von Barh et al. [42] used high-speed photography to study the partially wetting process. They found that the spreading laws depend on the fluid viscosity. The low-viscosity fluids spread over tens of milliseconds to reach equilibrium stage. The spreading radius approximately satisfies $R(t) \sim t^{0.5}$, however, the high viscosity fluids spreading with $R(t) \sim t^{0.1}$.

According to different time and length scale, there are five numerical simulation techniques, as shown in Fig. 1.4, the Ab initio method, the hybrid method of quantum molecular dynamic simulations and the classical molecular dynamics simulations, the classical molecular dynamics simulations (MD), the lattice

Fig. 1.4 Multiscale numerical simulation techniques



Boltzmann method (LBM), and the traditional Computational Fluid Dynamics (CFD) method. We do not need to consider the quantum effects during the dynamic wetting process, because, to some extent, wetting is a macroscopic process. However, the distinct drawback of CFD is significant when dealing with the dynamic wetting problems. On one hand, the evolutions of spreading radius and dynamic contact angle are inputted as boundary conditions in the CFD models when dealing with the wetting problems. Therefore, we could not study the dynamic wetting behaviors from CFD simulations. In addition, the non-slip boundary conditions used in the CFD methods are incapable to model the dynamic wetting process due to the “contact line paradox” as discussed in Sect 1.1 [2]. Molecular dynamics (MD) simulations have been recognized as a powerful tool in studying the contact line motion problems. However, most MD simulations focused on simple Lennard-Jones (LJ) fluid droplet spreading on LJ substrates, a system that is quite different from real dynamic wetting system and is hence impossible to mimic important physical properties (e.g., surface tension, density, and viscosity) of fluids which is related to the dynamic wetting [43–54]. The LBM is based on mesoscopic kinetic equations (the Boltzmann equation). The NS equations can be derived from the Boltzmann equation using the Chapman–Enskog multiscale expansion. Therefore, the LBM has been regarded as a very promising method to simulate the multiscale problems. Recently, a number of studies have used the LBM to analyze the flow and heat transfer of nanofluids using a single-component single-phase model [26–34] or a multicomponent single-phase model [35–38]. Due to the intrinsic microscopic kinetics, the LBM was widely used to investigate dynamic wetting [55–62]. However, most of these studies focused on the simple Newtonian fluid dynamic wetting.

In conclusion, the Newtonian dynamic wetting has been studied for almost 5 decades. Although the physical consensus is still unreached on the mechanism of contact line motion, a large amount of experimental data has been reported. Several theoretical models have been proposed to describe the relations of θ_D-U and $R-t$. Microscopic and mesoscopic scale simulation techniques have been established to study the dynamic wetting of Newtonian fluids.

1.2.2 Dynamic Wetting with Complex Surfaces and Complex External Physical Fields

Due to the complexity of dynamic wetting, the early studies usually focused on the dynamic wetting of simple fluids on an ideal smooth surface without any external physical fields. These studies can provide the fundamental understanding of dynamic wetting process, satisfying the curiosity of exploring the unknown world. However, it is hard to find simple fluids and ideal surfaces in the real world. Therefore, it is of greater practical interest to study the dynamic wetting of complex fluids on the real solid surface with external physical fields.

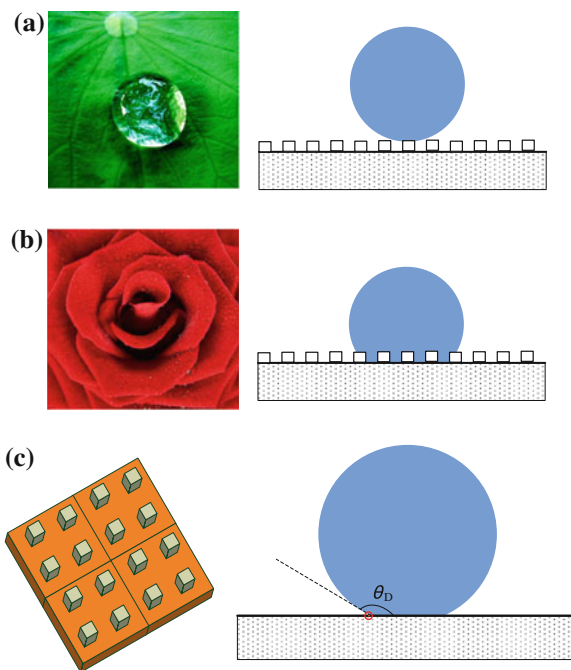
The goal of studying dynamic wetting is to tune the wettability or dynamic wetting behaviors of fluids on solid surfaces. Usually, tuning the solid surface properties is the most favorite option which draws extensive research interest. For a liquid drop on the smooth and ideal surfaces, the static contact angle is a single value, which can be determined by the Young's equation, $\cos \theta_Y = (\sigma_{SV} - \sigma_{SL}) / \sigma_{LV}$. However, for the real solid surfaces, a drop placed on a surface has a spectrum of contact angles ranging from the so-called advancing (maximal) contact angle, θ_A , to the so-called receding (minimal) contact angle, θ_R . The difference between these values, $\theta_A - \theta_R$, is known as contact angle hysteresis, which is usually attributed to the roughness or the heterogeneity of the solid surface [63–66]. The contact angle hysteresis is the fundamental guideline for the designs of various lotus biomimetic or nanostructured surfaces, with super-hydrophobic or super-hydrophilic characteristics [67–70], as shown in Fig. 1.5.

Other complex facts lie in that the dynamic wetting process usually takes place with various external physical fields, such as electric, magnetic, thermal, or optical fields [72–77]. The electrowetting [72], which is the modification of the wetting properties of a surface (which is typically hydrophobic) with an applied electric field, is one of the hot topics in this area. A specific example for the dynamic wetting with complex external fields is the liquid water transport within the gas diffusion layer in the proton exchange membrane (PEM) fuel cells, in which the dynamic wetting of liquid water occurs with the external electric field, electro-osmosis, and temperature gradient, as well as the complex porous structures. By tuning the wettability of gas diffusion layer, the output power of PEM fuel cells can be improved significantly [78].

1.2.3 Dynamic Wetting of Complex Fluids

The viscosity of Newtonian fluids is independent of the shear stress rate. However, for most of the fluids, especially for most of the mixture fluids, the viscosity depends on shear rate or shear rate history and exhibits non-Newtonian characteristics. Many polymer solutions and particulate suspensions are non-Newtonian fluids, as are many commonly found substances such as ketchup, custard,

Fig. 1.5 Dynamic wetting on the complex solid surfaces. **a** Lotus leaf effects. **b** Rose leaf effects. **c** Wettability on hybrid micro-nanostructural surfaces [71]



toothpaste, starch suspensions, paint, blood, and shampoo. There is extensive research of dynamic wetting with Newtonian fluids in the literature, but only a few theoretical and experimental studies have explored how non-Newtonian fluids spread over solid substrates. It is of greater practical interest to study the non-Newtonian fluid dynamic wetting. However, the study of non-Newtonian fluid dynamic wetting had just begun in the last two decades [71]. The current awareness of the non-Newtonian fluid dynamic wetting is far less than that of Newtonian fluid, which can be attributed to the complex nonlinear constitutive relations, or the diversity properties in non-Newtonian fluids.

The previous studies on non-Newtonian fluid dynamics wetting mainly focused on the relatively simple power-law fluids (shear-thinning and shear-thickening fluids). Carré and Woehl [79, 80] reported the dynamic wetting behaviors of shear-thinning fluids and derived a $\theta_D - U$ relation based on the “energy-balanced method” proposed by de Gennes’s [1]. They found that the $\theta_D - U$ strongly depends on the rheological index, n . However, Neogi and Ybarra [81] reported a contrary result that the $\theta_D - U$ relation was independent of the fluid rheology. They also used the energy-balanced method to build the $\theta_D - U$ relations of Ellis and Reiner-Rivlin fluids. The viscous dissipation was analyzed using approximative method because the constitutive relationships of these two fluids are of complexity. The authors suggested that the non-Newtonian fluid dynamic wetting can be described by Newtonian fluid $\theta_D - U$ relation, only changing the viscosity of the relation into the non-Newtonian fluid viscosity at zero shear rate.

Starov et al. [82] analyzed the complete wetting of power-law non-Newtonian fluids using the lubrication theory. Their results showed that the dynamic contact angle of the power-law fluid droplet was related to the droplet sizes during the dynamic wetting process, which was quite different from Newtonian fluids. In addition, for both the capillary and gravitational regimes, the spreading exponents of Newtonian fluids were higher than that of shear-thinning fluids, but lower than shear-thickening fluids.

Betelu and Fontelos [83, 84] also used the lubrication approximate to study the complete spreading of power-law droplet. They only considered the shear-thinning fluids in the capillary regime. The shape evolution of free surface was solved numerically using similarity transformation. Wang et al. [85, 86] established a two-dimensional model to describe the power-law fluid droplet spreading by solving the ordinary differential equations of film thickness using traveling wave transformation. Liang et al. [87, 88] established two power-law fluid dynamic wetting models based on the HD and MKT, which all agree well with the experimental data. Table 1.4 compares various non-Newtonian dynamic wetting models.

Compared with the Newtonian fluids, very few experimental data of the non-Newtonian fluid dynamic wetting have been reported. In addition, most of the experiments focused on the shear-thinning fluids, as shown in Table 1.5. Carré and Woehl [79] tested the shear-thinning fluid droplets (PDMS+silica and acrylic typographic ink) spreading on the glass slides, which agreed with their non-Newtonian fluid dynamic wetting model. Rafai and Bonn [89, 90] studied the shear-thinning (xanthan solution) and normal stress fluid (polyacrylamide solution) dynamic wetting on mica using the droplet spreading method. Their results show that the spreading exponents of the two types of fluids in their experiments are both less than 1/10, the spreading exponent of Newtonian fluids [91]. In addition, the exponent decreases with increasing solution concentrations due to the more prominent non-Newtonian behaviors. The results verified the Starov's finding that the spreading exponents of shear-thinning fluids should be less than that of Newtonian fluids. Wang and Duan's group [85, 86] have done many relevant works

Table 1.4 Theoretical studies of non-Newtonian dynamic wettings

Authors	Types of non-Newtonian fluids	Wettability	Models
Carré and Woehl [79, 80]	Shear thinning	Completely/partially	Hydrodynamics
Starov et al. [82]	Shear thinning/shear thickening	Completely	Hydrodynamics
Betelu et al. [83, 84]	Shear thinning	Completely/partially	Hydrodynamics
Wang et al. [85, 86]	Shear thinning	Completely/partially	Hydrodynamics
Liang et al. [87, 88]	Shear thinning/shear thickening	Completely/partially	Hydrodynamics/MKT

Table 1.5 Experiments on the non-Newtonian fluid dynamic wetting

Authors	Fluid types	Fluids/substrates	Methods
Carré and Woehl [79]	Power law	SiO ₂ -PDMS/glass	Droplet spreading
Rafai et al. [89, 90]	Power law	Xanthan/mica	Droplet spreading
Wang et al. [85, 86]	Shear thinning/shear thickening	Multiple fluids/multiple surfaces	Droplet spreading
Digilov [93]	Power law	Xanthan/capillary tube	Capillary rise
Min et al. [92]	Shear thinning	Multiple fluids/multiple surfaces	Droplet spreading/Wilhelmy plate dipping

on the non-Newtonian fluid dynamic wetting: they first studied the dynamic wetting behaviors using two experimental techniques, droplet spreading method and Wilhelmy plate method, corresponding to the spontaneous wetting and forced wetting, respectively; they extended the scope of complex fluids from power-law fluids to more complex fluids without general constructive relations; they proposed several theoretical models with pure HD, energy-balanced model, and the molecular kinetic theory; they also conducted multiscale simulation techniques, the mesoscopic LBM, and the microscopic MD simulations, to study the dynamic wetting behaviors of complex fluids. It is noted that they contributed several significant findings in the field of non-Newtonian fluid dynamic wetting. For example, by introducing a new defined capillary number (Ca), they integrated the present diverse non-Newtonian fluid dynamic wetting models into a general model; they also found that the dynamic wetting of non-Newtonian fluids strongly depends on the macrogeometry, which is quite different from the Newtonian fluids [92].

1.2.4 Studies of Dynamic Wetting by Nanofluids

Nanofluids, fluids containing suspension of nanometer-sized particles, can also be regarded as one type of complex fluids. Nanofluids are promising branches in nanotechnologies which manipulate matter with at least one dimension sized from 1 to 100 nm. Nanotechnology is able to create many new materials and devices with a vast range of applications, such as interface and colloid science, nanoscale materials, nanomedicine, nanoparticles, and biomedical applications. As part of this technology, nanofluids have also been widespread concerned. The concept of nanofluid was first proposed by Choi [94]. The nanofluids are designed to enhance thermal properties and/or reduce drag coefficients for application ranging from electronics cooling to microfluidics. The suspended nanoparticles can significantly

Table 1.6 Critical heat flux (CHF) in the nanofluid boiling

Authors	Nanofluids	CHF enhancement (%)
You et al. [111]	Al ₂ O ₃ /water	200
Kim et al. [112]	TiO ₂ /water	200
Vassallo et al. [113]	SiO ₂ /water	60
Tu et al. [114]	Al ₂ O ₃ /water	67
Kim and Kim [115]	TiO ₂ /water	50
Moreno et al. [116]	Al ₂ O ₃ /water, ZnO/water; Al ₂ O ₃ /silicone oil	200
Bang et al. [117]	Al ₂ O ₃ /water	50
Milanova et al. [118]	SiO ₂ /water, CeO/water, Al ₂ O ₃ /water	170
Jackson et al. [119]	Au/water	175
Wen and Ding [120]	Al ₂ O ₃ /water	40

modify the transport properties of the base fluids, and the resulting nanofluids exhibit attractive properties such as high thermal conductivity and high boiling heat transfer coefficient [95–102]. For example, with 1 % nanoparticle loading, the thermal conductivity of base fluid can be increased 40 % [100].

Recently, it is reported that nanofluids exhibit enhanced or tunable dynamic wetting characteristics compared with the base fluids [103–110]. The tunable wetting behaviors can be used to extend the applications of nanofluids into many areas such as fabricating functional surfaces with desired properties, enhancing heat transfer or reducing the drag in micro/biofluid systems, or enhancing boiling or condensation phase change in heat exchangers. In addition, the dynamic wetting by nanofluids also offers a new approach to tune the wettability of fluids on the solid surfaces, which is based on the fluids rather than the solid surfaces. This approach provides more options for us to tune the wettability of fluids on solid surfaces, because there are many tunable parameters in nanofluids, such as nanoparticle loading, material, size, shape, as well as the base fluid material. Thus, nanofluids may be smart materials if their wettability can be manipulated. Therefore, the dynamic wetting by nanofluids has become a hot topic in many areas, from thermal science, material science, to the colloidal and interfacial science.

The dynamic wetting by nanofluids attracted research attentions firstly by some interesting phenomena: Adding nanoparticles into base fluids can modify the equilibrium contact angle, change the surface tension, or result in the solid-like ordering structure of nanoparticles assembled near the contact line; anomalous evaporating or boiling behaviors by nanofluids [103, 107, 111–120]. These phenomena were found to be related to the different dynamic wetting behavior of nanofluids compared with their base fluids. One motivation of studying nanofluid dynamic wetting in the thermal engineering community lies in the enhancement of the heat transfer coefficient and the CHF [111–120] during the boiling process, as shown in Table 1.6.

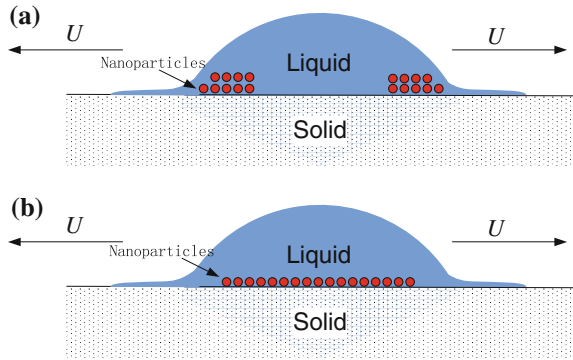
The enhancement in the liquid–vapor phase change was explained by the improvement of nanofluid dynamic wetting. Thus, the abnormal dynamic wetting behavior of nanofluids, especially the contact line motion affected by the addition nanoparticles, stimulates the research of nanofluid dynamic wetting. Through years of exploration work, researchers have been basically reached these consensuses: the dynamic wetting itself is a complex process; adding nanoparticles into base fluids will lead to more complex dynamic wetting by inducing the complicated nanoparticle random motion in the bulk liquid, or self-assembly at the liquid–vapor interface or in the solid–liquid–vapor three-phase contact line region; the process will be more unpredictable if the dynamic wetting occurs with phase change or complex external fields. The mechanism of nanofluid dynamic wetting is still unclear due to the lack of macroscopic and microscopic experiments and theories.

There are several explanations for the roles of adding nanoparticles in the dynamic wetting: (1) Adding nanoparticles into the base fluids was reported to change the dynamic wetting behaviors by modifying the rheological properties of nanofluids. The dynamic wetting is enhanced by shear-thinning nanofluids but is hindered by shear-thickening nanofluids [13]. (2) The heterogeneity due to the nanoparticle self-assembly also affects the dynamic wetting by nanofluids. Nanofluid “super-spreading” was reported by Wasan et al. [107] who found that an 8 nm micellar solution, an 1 μm latex suspension, and a 20 nm silica suspension were found to enhance the base fluids wettability [106–108]. A solid-like ordering structure of nanoparticles was observed near the contact line region using interferometry. This solid-like ordering structure stemming from the settlement and assembly of nanoparticles gives rise to a structural disjoining pressure in the vicinity of the contact line. This excess pressure in turn alters the force balance near the contact line and enhances the spreading of nanofluids. The super-spreading behavior of nanofluids induced by the self-assembly of the nanoparticles and the structural disjoining pressure have been widely used to explain the enhanced dropwise evaporation [18, 19] and CHF with nanofluids [20–23]. (3) Another explanation for the super-spreading by nanofluids was that nanoparticles were assumed to settle at the bottom of the droplet; thus, reducing the solid–liquid friction and, hence, facilitating the fluid spreading [103]. The last two explanations are schematically shown in Fig. 1.6. However, these two explanations are only qualitative assumptions; both adequate experimental evidences and theoretical descriptions are still needed.

1.3 Objectives of the Dissertation

According to the literature review, the mechanism of dynamic wetting by nanofluids is still unclear due to limitations of nanoscale experimental techniques and fundamental theories. Studies of the dynamic wetting by nanofluids are facing great challenges because the wetting behavior crosses several length and timescales. This study analyzes the effects of the bulk and local dissipation in the nanofluids due to

Fig. 1.6 Schematics of super-spreading due to nanoparticle self-assembly. **a** Self-assembly at the contact line region. **b** Bottom sedimentation



the nanoparticle transport and self-assembly on the macroscopic dynamic wetting behavior using macroscopic experiments and multiscale simulation methods. The results describe both the macroscopic and microscopic mechanisms and tunable methods to control nanofluid dynamic wetting. The research road map is shown in Fig. 1.7.

In Chap. 2, the contact line mobility and contact angle evolution were first measured using the droplet spreading method and the Wilhelmy plate method. The effects of the nanofluid parameters, such as nanoparticle loading, particle diameter, particle material, and base fluid, were examined, as well as the effects of the substrate material.

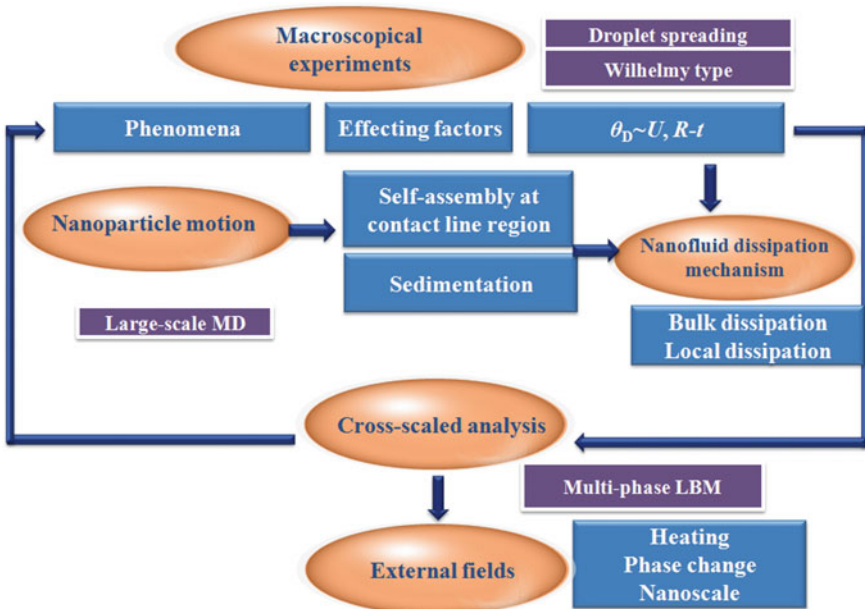


Fig. 1.7 Schematic of research road map

In Chaps. 3 and 4, MD simulations were then conducted to study the nanoparticle transport and self-assembly within the bulk liquid or at the interface, which affect the bulk dissipation and the local dissipation. The results describe the microscopic mechanisms by which the bulk dissipation affects the nanofluid surface tension, viscosity, and rheology. Without nanoparticle self-assembly at the contact line, nanofluid dynamic wetting was controlled by the increasing surface tension and the increasing solid–liquid friction coefficient. MD simulations of nano-thin-film motion quantitatively illustrate how the capillary force and the “structural disjoining pressure” drive the contact line motion.

In Chap. 5, a mesoscopic understanding of the nanofluid wetting kinetics was then obtained using the LBM. The objective of this chapter was examining the effects of two nanoparticle dissipations, the bulk dissipation and the local dissipation, on the macroscopic dynamic wetting process. The roles of surface tension, rheology, and the structural disjoining pressure were investigated.

In Chap. 6, the nanofluid dynamic wetting was studied with complex external conditions. The effects of substrate heating and intensive free surface evaporation on the wetting kinetics of nanofluids were simulated using MD simulations. The effects of initial droplet temperature, substrate temperature, and wettability were examined. The microscopic mechanisms of nanoparticle self-assembly and nanofluid droplet evaporating–spreading behavior were revealed by tracing the particle motion and molecular mobility near the contact line region.

Finally, in Chap. 7, we provided the general conclusions and the contributions of this book. The prospects in dynamic wetting by nanofluids were also provided in this chapter.

References

1. de Gennes PG (1985) Wetting: statics and dynamics. *Rev Mod Phys* 57:827–863
2. Huh C, Scriven LE (1971) Hydrodynamic model of steady movement of a solid-liquid-fluid apparent contact line. *J Colloid Interface Sci* 35:85–101
3. Dussan VEB (1979) On the shredding of liquids on solid surfaces: static and dynamic contact lines. *Annu Rev Fluid Mech* 11:317–400
4. Oron A, Davis SH, Bankoff SG (1997) Long-scale evolution of thin liquid films. *Rev Mod Phys* 69:931–980
5. Kistler SF (1993) Hydrodynamics of wetting. In: Berg JC (ed) *Wettability*. Marcel Dekker, New York, pp 311–429
6. Petrov PG, Petrov JG (1992) A combined molecular-hydrodynamic approach to wetting kinetics. *Langmuir* 8:1762–1767
7. Hayes RA, Ralston J (1993) Forced liquid movement on low-energy surfaces. *J Colloid Interface Sci* 159:429–438
8. Hayes RA, Ralston J (1994) The molecular-kinetic theory of wetting. *Langmuir* 10:340–342
9. de Ruijter MJ, De Coninck J, Blake TD (1997) Contact angle relaxation during the spreading of partially wetting drops. *Langmuir* 13:7293–7298
10. de Ruijter MJ, de Coninck J, Oshanin G (1999) Droplet spreading: partial wetting regime revisited. *Langmuir* 15:2209–2216

11. Schneemilch M, Hayes RA, Petrov JG (1998) Dynamic wetting and dewetting of a low-energy surface by pure liquids. *Langmuir* 14:7047–7051
12. Blake TD, Bracke M, Shikhmurzaev YD (1999) Experimental evidence of nonlocal hydrodynamic influence on the dynamic contact angle. *Phys Fluids* 11:1995–2007
13. de Ruijter MJ, Charlot M, Voue M (2000) Experimental evidence of several time scales in drop spreading. *Langmuir* 16:2363–2368
14. Blake TD, Shikhmurzaev YD (2002) Dynamic wetting by liquids of different viscosity. *J Colloid Interface Sci* 253:196–202
15. Hocking LM (1976) A moving fluid interface on a rough surface. *J Fluid Mech* 76:801–817
16. Huh C, Mason SG (1977) Steady movement of a liquid meniscus in a capillary tube. *J Fluid Mech* 81:401–419
17. Hocking LM (1977) A moving fluid interface, Part II: the removal of the force singularity by a slip flow. *J Fluid Mech* 79:209–229
18. Dussan VEB (1976) The moving contact line: the slip boundary conditions. *J Fluid Mech* 76:665–684
19. Lowndes J (1980) The numerical simulation of the steady movement of fluid meniscus in a capillary tube. *J Fluid Mech* 101:631–646
20. Bach P, Hassager O (1985) An algorithm for the use of the Lagrangian specification in Newtonian fluid mechanics and applications to free-surface flow. *J Fluid Mech* 152:173–190
21. Ludviksson V, Lightfoot EN (1968) Deformation of advancing menisci. *AIChE J* 14:674–677
22. Tanner LH (1979) The spreading of silicone oil drops on horizontal surfaces. *J Phys D* 12:1473–1484
23. Hervet H, de Gennes PG (1984) The dynamics of wetting: precursor films in the wetting of dry solids. *C R Acad Sci* 299:499–503
24. Blake TD (1993) Dynamic contact angles and wetting kinetics. In: Berg JC (ed) *Wettability*. Marcel Dekker, New York, pp 251–309
25. Daniel RC, Berg JC (2006) Spreading on and penetration into thin, permeable print media: application to ink-jet printing. *Adv Colloid Interface Sci* 123:439–469
26. Cox RG (1986) The dynamics of the spreading of liquids on a solid surface I. Viscous flow. *J Fluid Mech* 168:169–194
27. Zhou MY, Sheng P (1990) Dynamics of immiscible-fluid displacement in a capillary tube. *Phys Rev Lett* 64:882–885
28. Sheng P, Zhou MY (1992) Immiscible-fluid displacement: contact-line dynamics and the velocity-dependent capillary pressure. *Phys Rev A* 45:5694–5708
29. Petrov JG, Ralston J, Schneemilch M et al (2003) Dynamics of partial wetting and dewetting in well-defined systems. *J Phys Chem B* 107:1634–1645
30. Voinov OV (1976) Hydrodynamics of wetting. *Fluid Dyn* 11:714–721
31. de Gennes PG (1986) Deposition of Langmuir-Blodgett layers. *Colloid Polym Sci* 264:463–465
32. Brochard-Wyart F, de Gennes PG (1994) Spreading of a drop between a solid and a viscous polymer. *Langmuir* 10:2440–2443
33. Brochard-Wyart F, Debrégeas G, de Gennes PG (1996) Spreading of viscous droplets on a non viscous liquid. *Colloid Polym Sci* 274:70–72
34. White FM (1998) *Fluid mechanics*. Mcgraw-Hill College, New York
35. Blake TD, Haynes JM (1969) Kinetics of liquid/liquid displacement. *J Colloid Interface Sci* 30:421–423
36. Blake TD, De Coninck J (2002) The influence of solid-liquid interactions on dynamic wetting. *Adv Colloid Interface Sci* 96:21–36
37. Glasstone S, Laidler KJ, Eyring H (1941) *The theory of rate processes*. McGraw-Hill, New York
38. Vega MJ, Gouttière C, Seveno D (2007) Experimental investigation of the link between static and dynamic wetting by forced wetting of nylon filament. *Langmuir* 23:10628–10634

39. Ray S, Sedev R, Priest C (2008) Influence of the work of adhesion on the dynamic wetting of chemically heterogeneous surfaces. *Langmuir* 24:13007–13012
40. de Ruijter M, Kölsch P, Voué M (1998) Effect of temperature on the dynamic contact angle. *Colloid Surface: A* 144:235–243
41. Wang X, Chen LQ, Bonaccorso E (2013) Dynamic wetting of hydrophobic polymers by aqueous surfactant and superspreader solutions. *Langmuir* 29:14855–14864
42. von Bahr M, Tiberg F, Yaminsky V (2001) Spreading dynamics of liquids and surfactant solutions on partially wettable hydrophobic substrates. *Colloids Surf A* 193:85–96
43. Koplik J, Banavar JR, Willemsen JF (1988) Molecular dynamics of poiseuille flow and moving apparent contact lines. *Phys Rev Lett* 60:1282–1285
44. Thompson PA, Robbins MO (1989) Simulations of ACL motion: slip and dynamic contact angle. *Phys Rev Lett* 63:766–769
45. Yang JX, Koplik J, Banavar JR (1991) Molecular dynamic of droplet spreading on a solid surface. *Phys Rev Lett* 67:3539–3542
46. Blake TD, Clarke A, de Coninck J et al (1997) Contact angle relaxation during droplet spreading: comparison between molecular kinetic theory and molecular dynamics. *Langmuir* 13:2164–2166
47. Liu H, Chakrabarti A (1999) Molecular dynamics study of adsorption and spreading of a polymer chain onto a flat surface. *Polymer* 40:7285–7293
48. Hwang CC, Ho JR, Lee RC (1999) Molecular dynamics of a liquid drop spreading in a corner formed by two planar substrates. *Phys Rev E* 60:5693–5698
49. Yaneva J, Milchev A, Binder K (2003) Dynamics of a spreading nanodroplet: a molecular dynamic simulation. *Macromol Theory Simul* 12:573–581
50. He G, Hadjiconstantinou NG (2003) A molecular view of Tanner’s law: molecular dynamics simulations of droplet spreading. *J Fluid Mech* 497:123–132
51. Shen YY, Couzis A, Koplik J et al (2005) Molecular dynamics study of the influence of surfactant structure on surfactant-facilitated spreading of droplets on solid surfaces. *Langmuir* 26:12160–12170
52. Bertrand E, Blake TD, de Coninck J (2005) Spreading dynamics of chain-like monolayers: a molecular dynamics study. *Langmuir* 21:6628–6635
53. Kim HY, Qin Y, Fichthorn KA (2006) Molecular dynamics simulation of nanodroplet spreading enhanced by linear surfactants. *J Chem Phys* 125:174708
54. Seveno D, Dinter N, de Coninck J (2010) Wetting dynamics of drop spreading: new evidence for the microscopic validity of the molecular-kinetic theory. *Langmuir* 26:14642–14647
55. Yang YT, Lai FH (2011) Numerical study of flow and heat transfer characteristics of alumina-water nanofluids in a microchannel using the lattice Boltzmann method. *Int Commun Heat Mass* 38:607–614
56. Kumar S, Prasad SK, Banerjee J (2010) Analysis of flow and thermal field in nanofluid using a single phase thermal dispersion model. *Appl Math Model* 34:573–592
57. Nemati H, Farhadi M, Sedighi K et al (2010) Lattice Boltzmann simulation of nanofluid in lid-driven cavity. *Int Commun Heat Mass* 37:1528–1534
58. Xuan YM, Li QA (2009) Energy transport mechanisms in nanofluids and its applications. In: 7th International conference on nanochannels and minichannels. Pohang, South Korea
59. Xuan YM, Yu K, Li Q (2005) Investigation on flow and heat transfer of nanofluids by the thermal lattice Boltzmann model. *Prog Comput Fluid Dy* 5:13–19
60. Xuan YM, Yao ZP (2005) Lattice Boltzmann model for nanofluids. *Heat Mass Transfer* 41:199–205
61. Khiabani RH, Joshi Y, Aidun C (2007) Convective heat transfer in a channel in the presence of solid particles. In: 7th ASME/JSME thermal engineering and summer heat transfer conference. Vancouver, Canada
62. Khiabani RH, Joshi Y, Aidun C (2010) Heat transfer in microchannels with suspended solid particles: lattice-Boltzmann based computations. *J Heat Transfer* 041003-1-9
63. Wenzel RN (1936) Resistance of solid surfaces to wetting by water. *Ind Eng Chem* 28:988–994

64. Cassie ABD (1948) Contact angle hysteresis on heterogeneous surfaces. *Discuss Faraday Soc* 3:11–16
65. Joanny JF, de Gennes PG (1984) A model for contact angle hysteresis. *J Chem Phys* 81:552–562
66. Schwartz LW, Garoff S (1985) Contact angle hysteresis and the shape of the three phase line. *J Colloid Interface Sci* 106:422–437
67. Quéré D (2005) Non-sticking drops. *Rep Prog Phys* 68:2495–2532
68. Dietrich S, Popescu MN, Rauscher M (2005) Wetting on structured substrates. *J Phys-Condens Mat* 17:S577–S593
69. Bruschi L, Kuhne H, Thiele U et al (2002) Dewetting of thin films on heterogeneous substrates: pinning versus coarsening. *Phys Rev E* 66:011602
70. Darhuber AA, Troian SM, Reisner WW (2001) Dynamics of capillary spreading along hydrophilic microstrips. *Phys Rev E* 64:031603
71. Bonn D, Eggers J, Indekeu J et al (2009) Wetting and spreading. *Rev Mod Phys* 81:739–805
72. Quilliet C, BERGE B (2001) Electrowetting: a recent outbreak. *Curr Opin Colloid Interface Sci* 6:34–39
73. Sondag-Huethorst JAM, Fokkink LGJ (1994) Potential-dependent wetting of electroactive ferricene-terminated alkanethiolate monolayers on gold. *Langmuir* 10:4380–4387
74. Verheijen HJJ, Prins MWJ (1999) Contact angle and wetting velocity measured electrically. *Rev Sci Instrum* 70:3668–3673
75. Blake TD, Clarke A, Stattersfield EH (2000) An investigation of electrostatic assist in dynamic wetting. *Langmuir* 16:2928–2935
76. Pollack MG, Fair RB, Shenderov A (2000) Electrowetting-based actuation of liquid microdroplets for microfluidic applications. *Appl Phys Lett* 77:1725–1726
77. Vallet M, Vallade M, BERGE B (1999) Limiting phenomena for the spreading of water on polymer films by electrowetting. *Eur Phys J B* 11:583–591
78. Pai YH, Ke JH, Huang HF (2006) CF₄ plasma treatment for preparing gas diffusion layers in membrane electrode assemblies. *J Power Sources* 161:275–281
79. Carré A, Woehl P (2002) Hydrodynamic behavior at the triple line of spreading liquids and the divergence problem. *Langmuir* 18:3600–3603
80. Carré A, Woehl P (2006) Spreading of silicon oils on glass in two geometries. *Langmuir* 22:134–139
81. Neogi P, Ybarra RM (2001) The absence of a rheological effect on the spreading of small drops. *J Chem Phys* 115:7811–7813
82. Starov VM, Tyatyushkin AN, Velarde MG et al (2003) Spreading of non-Newtonian liquids over solid substrates. *J Colloid Interface Sci* 257:284–290
83. Betelu SI, Fontelos MA (2003) Capillarity driven spreading of power-law fluids. *Appl Math Lett* 16:1315–1320
84. Betelu SI, Fontelos MA (2004) Capillarity driven spreading of circular drops of shear-thinning fluid. *Math Comput Model* 40:729–734
85. Wang XD, Lee DJ, Peng XF et al (2007) Spreading dynamics and dynamic contact angle of non-Newtonian fluids. *Langmuir* 23:8042–8047
86. Wang XD, Zhang Y, Lee DJ et al (2007) Spreading of completely wetting or partially wetting power-law fluid on solid surface. *Langmuir* 23:9258–9262
87. Liang ZP, Wang XD, Lee DJ et al (2009) Spreading dynamics of power-law fluid droplets. *J Phys: Condens Matter* 21:464117
88. Liang ZP, Wang XD, Duan YY et al (2010) Dynamic wetting of non-Newtonian fluids: multicomponent molecular-kinetic approach. *Langmuir* 26:14594–14599
89. Rafai S, Bonn D, Boudaoud A (2004) Spreading of non-Newtonian fluids on hydrophilic surfaces. *J Fluid Mech* 513:77–85
90. Rafai S, Bonn D (2005) Spreading of non-Newtonian fluids and surfactant solutions on solid surfaces. *Phys A* 358:58–67
91. Hoffman RL (1975) Study of advancing interface 1. Interface shape in liquid-gas systems. *J Colloid Interface Sci* 50:228–241

92. Min Q, Duan YY, Wang XD et al (2010) Spreading of completely wetting, non-Newtonian fluids with non-power-law rheology. *J Colloid Interface Sci* 348:250–254
93. Digilov RM (2008) Capillary rise of a non-Newtonian power law liquid: Impact of the fluid rheology and dynamic contact angle. *Langmuir* 24:13663–13667
94. Choi SUS (1995) Enhancing thermal conductivity of fluids with nanoparticle. In: Wang HP, Siginer DA (eds) ASME, FED 231/MD-66. New York
95. Hu ZS, Dong JX (1998) Study on antiwear and reducing friction additive of nanometer titanium oxide. *Wear* 216:92–96
96. Hamilton RL, Crosser OK (1962) Thermal conductivity of heterogeneous two component system. *Ind Eng Chem Fundam* 1:187–191
97. Lee S, Choi SUS, Li S (1999) Measuring thermal conductivity of fluids containing oxide nanoparticles. *J Heat Transfer* 121:280–289
98. Nagasaka Y, Nagashima A (1981) Absolute measurement of the thermal conductivity of electrically conducting liquids by the transient hot-wire method. *J Phys E: Sci Instrum* 14:1435–1440
99. Wang XW, Xu XF, Choi SUS (1999) Thermal conductivity of nanoparticle-fluid mixture. *J Thermophys Heat Transfer* 13:474–480
100. Sarit KD, Nandy P, Peter T (2003) Temperature dependence of thermal conductivity enhancement for nanofluids. *J Heat Transfer* 125:567–574
101. Murshed SMS, Leong KC, Yang C (2008) Investigations of thermal conductivity and viscosity of nanofluids. *Int J Therm Sci* 47:560–568
102. Das SK, Putra N, Roetzel W (2003) Pool boiling characteristics of nano-fluids. *Int J Heat Mass Transfer* 46:851–862
103. Sefiane K, Skilling J, MacGillivray J (2008) Contact line motion and dynamic wetting of nanofluid solutions. *Adv Colloid Interface Sci* 138:101–120
104. Vafaei S, Borca-Tasciuc T, Podowski MZ et al (2006) Effect of nanoparticles on sessile droplet contact angle. *Nanotechnology* 17:2523–2527
105. Trokhymchuk A, Henderson D, Nikolov AD et al (2001) A simple calculation of structural and depletion forces for fluids/suspensions confined in a film. *Langmuir* 17:4940–4947
106. Chaudbury MJ (2003) Spread the word about nanofluids. *Nature* 423:131–132
107. Wasan DT, Nikolov AD (2003) Spreading of nanofluids on solids. *Nature* 423:156–159
108. Chengara A, Nikolov AD, Wasan DT et al (2006) Spreading of nanofluids driven by the structural disjoining pressure gradient. *J Colloid Interface Sci* 280:192–201
109. Choi CH, Kim CJ (2006) Large slip of aqueous liquid flow over a nanoengineered superhydrophobic surface. *Phys Rev Lett* 96:066001
110. Sefiane K, Bennacer R (2009) Nanofluids droplets evaporation kinetics and wetting dynamics on rough heated substrates. *Adv Colloid Interface Sci* 147–148:263–271
111. You SM, Kim J, Kim KH (2003) Effect of nanoparticles on critical heat flux of water in pool boiling heat transfer. *Appl Phys Lett* 83:3374–3376
112. Kim H, Kim J, Kim M (2006) Experimental study on CHF characteristics of water-TiO₂ nano-fluids. *Nucl Eng Technol* 38:619–623
113. Vassallo P, Kumar R, Amico SD (2004) Pool boiling heat transfer experiments in silica-water nano-fluids. *Int J Heat Mass Transfer* 47:407–441
114. Tu JP, Dinh N, Theofanous T (2004) An experimental study of nanofluid boiling heat transfer. In: Proceedings of sixth international symposium on heat transfer. Beijing, China
115. Kim HD, Kim MH (2009) Critical heat flux behavior in pool boiling of water-TiO₂ nano-fluids. In: Proceedings of fourth japan-korea symposium on nuclear thermal hydraulics and safety. Sapporo, Japan
116. Moreno M, Oldenburg S, You SM et al (2005) Pool boiling heat transfer of alumina-water, zinc oxide-water and alumina-water ethylene glycol nanofluids. In: Proceedings of HT 2005. San Francisco, California
117. Bang IC, Chang SC (2005) Boiling heat transfer performance and phenomena of Al₂O₃-water nano-fluids from a plain surface in a pool. *Int J Heat Mass Transfer* 48:2407–2419

118. Milanova D, Kumar R, Kuchibhatla S et al (2006) Heat transfer behavior of oxide nanoparticles in pool boiling experiment. In: Proceedings of the fourth international conference on nanochannels, microchannels and minichannels. Limerick, Ireland
119. Jackson JE, Borgmeyer BV, Wilson CA et al (2006) Characteristics of nucleate boiling with gold nanoparticles in water. In: Proceedings of IMECE-2006. Chicago
120. Wen D, Ding Y (2005) Experimental investigation into the pool boiling heat transfer of aqueous based alumina nanofluids. *J Nanopart Res* 7:265